Investigation of Siderophile Behavior and Tungsten Systematics in Ordinary Chondrites

Tytrice Faison
Dr. Richard Ash
GEOL394

Abstract

Ordinary chondrites are meteorites derived from silicate-rich, primitive asteroids. They are commonly referenced to provide insight into the early Solar System. One such example is the timing of core formation, which can be derived from Hf-W radiometric dating. Ordinary chondrites contain metal in varying amounts, so they can be useful for constraining processes that involve the diffusion of siderophile elements. A study conducted by Archer et al. (2019) analyzed four H5 ordinary chondrites; two produced different Hf-W closure ages depending on the size of the metal grains and the other two produced consistent ages. To understand the role of grain size in the diffusion of tungsten, this study investigated the behavior of siderophile elements under a range of petrologic conditions and grain sizes via laser ablation analysis. We found that while siderophile elements preferentially diffuse into small grains (<150 microns), W will preferentially diffuse into either taenite or kamacite as a result of the oxygen fugacity within the parent body. This may have an effect on the measured Hf-W closure age, such as seen in the Archer et al. (2019) study.

Introduction

Our solar system started when a nebula of dust and gas collapsed under gravitational forces into a protoplanetary disk due to angular momentum (Bouvier et al., 2010). Cosmic sediments from that disk experienced heating and cooling sequences as they accreted into planets and planetesimals. The Solar System was formed about 4.5 billion years ago, and the cores of terrestrial planets took about 50 million years to form (Montmerle et al., 2006). This formation was accompanied by processes such as core differentiation, and frequent heating and cooling events that metamorphosed terrestrial objects. Meteorites are used to study early Solar System processes because their parent bodies, which are typically asteroids, have remained largely geologically unprocessed and chemically isolated since their formation in the protoplanetary disk. There are various types of chondritic and non-chondritic meteorites, each providing important insights into early Solar System formation, but this study will focus on ordinary chondrites.

Ordinary chondrites are silicate-rich meteorites composed of nebular material from the early protoplanetary disk. They are also the most commonly found meteorites on Earth (Vernazza et al., 2014). Ordinary chondritic meteorites are categorized as H, L, or LL depending on the amount of total iron in the composition. H chondrites have the most total iron, L chondrites have less total iron, and LL chondrites have the least total iron (see Table 1. below). The weight percent of Fe in equilibrated ordinary chondrites is about 28% in H chondrites, 22% in L chondrites, and 19% in LL chondrites (Vernazza et al., 2014).

	H	L	LL
Fall statistics (%)	34	37	9
Fe (wt%)	28	22	19
Fe/Si (atomic)	0.81	0.57	0.52
Metal (vol%)	8.4	4.1	2
Fa content of olivine*	16-20	21-26	27-31
Fs content of pyroxene*	15-17	18-22	22-30
~$\Delta^{17}O$ (‰)**	0.7	1.1	1.3
Ol / (Ol + Px)*	51-60	60-67	70-82

Table 1. Example Properties of Equilibrated Ordinary Chondrites sourced from Vernazza et al. (2019). The table records differences in iron concentration between H, L, and LL ordinary chondrites, as well as other compositional differences.

Ordinary chondrites also contain iron in multiple oxidation states and therefore contain different phases, *i.e.*, the iron can be in a metallic phase (Fe^0) or in the silicate phase (Fe^{2+}). H chondrites contain a higher proportion of metallic iron (Fe^0) than L or LL chondrites. Conversely, LL chondrites contain more oxidized iron (Fe^{2+}) than LL or H chondrites. Therefore, the dominant oxidation state of iron varies with petrologic type, *i.e.*, H chondrites are the most reduced samples and LL chondrites are the most oxidized. Ordinary chondrites are also categorized from type 3 to 6 according to the degree of thermal metamorphism the sample has experienced. Type 3 correlates to the lowest degree of thermal metamorphism, and type 6 correlates to the highest degree. Type 1 and 2 refer to metamorphism involving water, and are reserved for carbonaceous chondrites--not ordinary chondrites (Grossman et al., 2005). (See Fig. 1) In the progression from type 3 to type 6, there are distinct textural changes, such as the relative amount of matrix and the size of crystal grains (Huss et al., 2006)

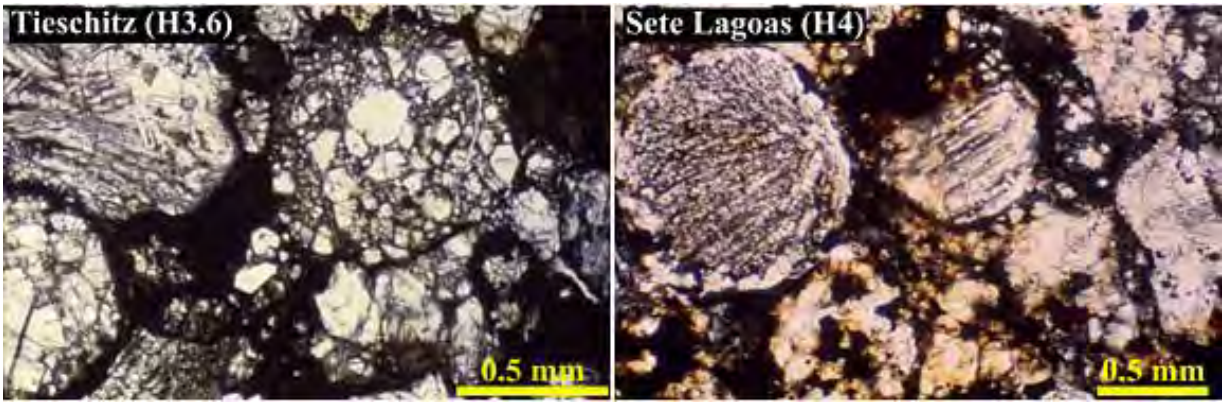

Figure 1. Reflected light photomicrographs sourced from Gary Huss. The image on the left is of an H3 chondrite (Tieschitz), and the image on the right is of an H4 chondrite (Sete Lagoas).

Ordinary chondrites also contain siderophile elements which can be used to constrain the timing of core formation, which led to HSE fractionation from silicate crust and mantle (Horan et al., 2009). Given their primitive origins, ordinary chondrites are ideal candidates for ^{182}Hf-^{182}W dating ($t_{1/2}$ = 8.9 Myr); a radiogenic process which is used to date the timing of core formation in terrestrial planets and other planetary bodies. Short-lived nuclides are optimal for dating processes that occurred within a relatively short time frame during the early Solar System because they can provide a high-resolution time scale for comparison (Holst et al., 2013). Hafnium (Hf) is lithophile, so it prefers to reside in silicates while tungsten (W) is moderately siderophile, so it preferentially resides in iron metal (Vernazza et al., 2014). As Hf decays to W, the difference in chemical affinity causes W to preferentially diffuse out of the silicate and into the metallic grains. The radiogenic process of ^{182}Hf-^{182}W can be used to study the internal structure and thermal history of ordinary chondrites (Hellman et al., 2019).

The diffusion of tungsten between metallic and non-metallic grains is reliant on energy from thermal activity, so there is a general assumption that the degree of tungsten equilibration is related to the chondrite's metamorphic type (3-6), as this classification reflects the degree of thermal metamorphism, *i.e.,* the time duration and temperature of heating. A study conducted by Archer et al. (2019) found that these assumptions may not show the entire picture. In their study, they analyzed 4 H5 chondrites by separating

magnetic (metal) and non-magnetic (silicate) material. They then measured the isotopes to calculate Hf-W closure ages. The data measured in two of those chondrites were similar for both small (<150 microns) and large (>150 microns) metal grains, however, in the other two chondrites, the small and large grains displayed different closure ages (Fig.2).

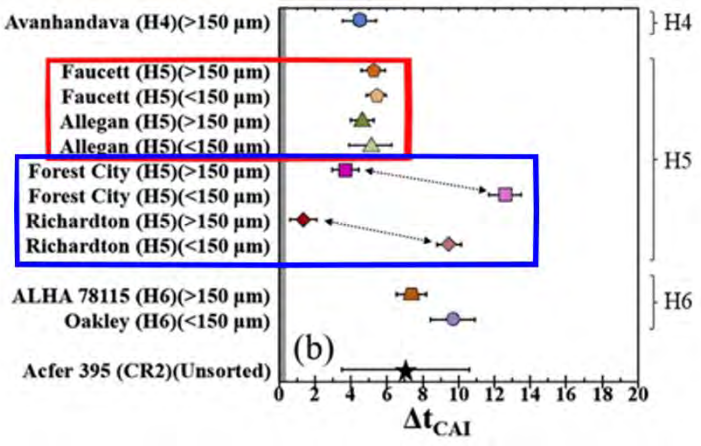

Figure 2. Hf-W Ages for H and CR Chondrites (Ma) sourced from Archer et al. (2019). Highlighted in the red box are the calculated closure ages of two H5 chondrites (Allegan and Faucett) where grains below and over 150 microns displayed similar degrees of tungsten diffusion. Highlighted in the blue box are the calculated closure ages of another two H5 chondrites (Richardton and Forest City) where the ages differ depending on grain size.

As a possible explanation, they stated:

> *"It is possible that in these meteorites [Forest City and Richardton], the <150 micron metal grains continued to efficiently exchange W with surrounding silicates/oxides at lower temperatures than >150 micron metal grains, possibly due to having larger surface area to volume ratios." (Archer et al., 2019)*

We have conducted an investigation to test this suggestion by Archer et al. by focusing on tungsten behavior and the systematics of siderophile elements. Our hypotheses are the following:

I. *Siderophile elements in ordinary chondrites that have experienced a higher degree of thermal metamorphism will be more equilibrated than those that experienced less thermal metamorphism.*
II. *Metal grains that have a higher surface-area/volume ratio, will contain more tungsten than metal grains with a lower ratio.*

Heat accelerates the motion of atoms, so we predicted that chondrites that have been exposed to higher degrees of thermal metamorphism will be more equilibrated than chondrites that experienced less thermal activity. Ordinary chondrites are classified according to the degree of thermal metamorphism acted upon the parent body. Therefore, according to hypothesis I, high metamorphic grade chondrites (type 6) will be the most equilibrated. This was tested by analyzing ordinary chondrites that range in metamorphic grade (type 4-6). Hypothesis II refers to the role of metallic grain size in the diffusion of tungsten. The Archer et al. (2019) study suggested that smaller grains can exchange tungsten at lower temperatures than big grains due to their size. Therefore, we predicted that small metal grains will contain more tungsten (and other siderophile elements) than large metallic grains. This was tested by measuring the width of every grain analyzed and comparing the trace element abundances of each size category.

This study investigated the behavior of tungsten, along with other siderophile and highly siderophile elements, under a range of metamorphic conditions to understand the role of grain size in the diffusion of tungsten in ordinary chondrites. Though the hypotheses are focused on tungsten, it was useful to measure other siderophile elements as well because their data gave context and provided a reference to compare to tungsten behavior.

Methods: Preparation, Analysis, Interpretation

The methods used in this study can be separated into three stages: preparation, analysis, and interpretation. The preparation stage describes the collection of samples as well as the photography of each individual grain. The analysis stage describes the process of laser-ablation and data collection, which was then used in the interpretation stage to create graphs that illustrate trends.

Preparation

The ordinary chondrites used in this study include NWA13290 (H6), Gao-Guenie (H5), Buzzard Coulee (H4), Vinales (L6), Mt. Tazerait (L5), Kendleton (L4), Bensour (LL6), Chelyabinsk (LL5), and NWA6080 (LL4) as listed in Figure 3. Analyzing a matrix of samples that range in thermal metamorphism and iron concentration allowed us to observe patterns of tungsten behavior under a series of conditions. All the samples were mounted in epoxy resin and polished. After all the chondrites were prepared, they were viewed under a microscope to understand their petrology and mineral distribution, and to search for suitable metal grains for analysis. Multiple photomicrographs were taken to provide a reference for documenting the grains selected for laser-ablation and for recording the exact position of each grain within each chondrite (see Fig. 4 below). These photographs were also used to record size measurements for each grain that was analyzed.

Bensour	Chelyabinsk	NWA6080
LL	LL	LL
6	5	4

Vinales	Mt. Tazerait	Kendleton	Sample
L	L	L	Class
6	5	4	Type

NWA13290	Gao-Guenie	Buzz. Coulee
H	H	H
6	5	4

Figure 3. Ordinary Chondrite Samples *The chondrites listed in this table will serve as subjects for the investigation. In total, 9 samples were analyzed which range between H, L, and LL, and type 4 to type 6.*

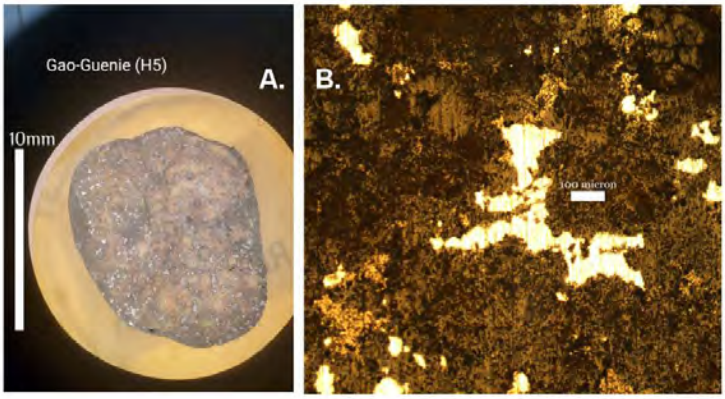

Figure 4. Photographs of the Gao-Guenie (H5) chondrite. *The figure to the left (A) was taken through the lens of an optical microscope. The figure to the right (B) is a photomicrograph of a metal grain (pale yellow) within Gao-Guenie next to a 100 micron scale bar.*

Analysis

For major, minor, and trace element measurements, an Element-2 ICP-MS coupled to a New Wave UP213 laser was used. The New Wave laser provides a beam of UV light (wavelength 213 nm) which was used to ablate the surface of each grain. The laser spot diameter we used ranged between 30-80 microns depending on the size of the grain. The energy of the laser was controlled to be between ~2.5-4.0 Jcm^{-2} and the laser fired at a frequency of 10Hz. Larger grains had multiple site analyses to search for elemental zoning of trace elements on the edge versus the center. The ablated material was transported to the ICP-MS via a stream of helium whereupon it was injected into the argon plasma for ionization. The isotopes observed in order of increasing mass include ^{57}Fe, ^{59}Co, ^{61}Ni, ^{63}Cu, ^{69}Ga, ^{73}Ge, ^{75}As, ^{97}Mo, ^{99}Ru, ^{103}Rh, ^{105}Pb, ^{183}W, ^{185}Re, ^{189}Os, ^{193}Ir, ^{195}Pt, and ^{197}Au. Detection limits are dependent upon the element being analyzed and the size of the spot being ablated, but the Element 2 can measure down to the parts per billion (ppb) range. Data processing was done via the LAMTRACE program. Raw abundances were CI normalized and FeS was assumed to be stoichiometric (Fe+Ni+Co = 100%).

Interpretation

Using data processing mechanics, CI (chondrite) normalized graphs and tables containing the trace element abundances of each grain were created. Two major types of graphs were used; one plots the abundance of each individual grain, the other plots the average abundance of all the grains. Using these graphs, trends in element abundance between petrologic types (H vs. L vs. LL and type 4 vs. 5 vs. 6) can be used to investigate how tungsten behaves under a series of thermal conditions and metallic iron abundances. Using the records of grain width and scale, element abundance data can be separated into grain size categories. The trends within each size category were then compared to learn whether grain size had any significant effect on the equilibration of each chondrite. Many of the analyzed metal grains within each chondrite are round, so the process of determining its size (width) is straightforward. The data from these “idealized” grains was isolated and highlighted as information regarding their surface-volume ratios are more accurate than data collected from irregularly shaped grains.

Results: Petrologic Type, Fe-Ni Alloys, Grain Size

Petrologic Type

Several general patterns have been observed between the chondritic petrologic types. The normalized abundance of trace siderophile elements in the metal grains within H chondrites tend to be more uniform than L or LL chondrites. Specifically, the abundance of each siderophile element is generally consistent between different metal grains in the H chondrites (Fig. 5C). The abundance of trace siderophile elements in the metal grains of H chondrites also tend to be more uniform in relative abundance. In the case of the H6 chondrite, the trendlines are relatively flat. The uniformity of H chondrites could be an indication that the metal grains in this petrologic type have a network of communication, evenly diffusing trace elements between grains. This explanation is further supported by the observation that the metal grains in H chondrites tend to be around the same size.

If we compare the abundance graphs between H, L, and LL chondrites (Fig. 5), the metal grains in L and LL chondrites seem to contain a higher abundance of siderophile elements than H chondrites, despite H chondrites containing more iron. However, it is important to remember that H chondrites contain more metal grains in general. So, it is still plausible to say that H chondrites contain more iron, and therefore a higher abundance of siderophile elements, in entirety.

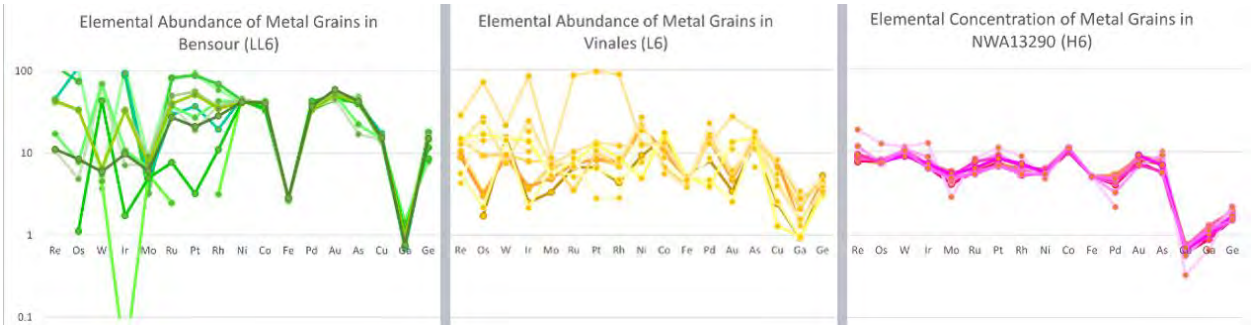

Figure 5. Trace Element Abundance of Metal Grains in H, L, and LL Chondrites. *These are logarithmic plots that record CI normalized abundance of siderophile elements in order of increasing volatility from left to right. Each line characterizes an individual grain. Green = LL, Yellow = L, Pink = H. All of the above chondrites are type 6.*

While H chondrites tend to have the most uniform trace element abundances, the L and LL chondrites measured have varied results (Fig. 5A and B). Another observation is that the metal grains in chondrites of lower metamorphic grades tend to have more variation in the abundance of siderophile elements than higher metamorphic grades (Fig. 6), with a few exceptions that will be discussed later. This is an indication that thermal metamorphism can aid in the diffusion of siderophile elements towards equilibrium. It is also noticeable that the abundances of refractory siderophile elements tend to have more variation than volatile elements. For example, in the chondrite Bensour (LL6) pictured in Fig. 5, the abundance of refractory elements Re, Os, and Ir range from 0-140 while the volatile elements Fe, Au, and Cu range from 2-60.

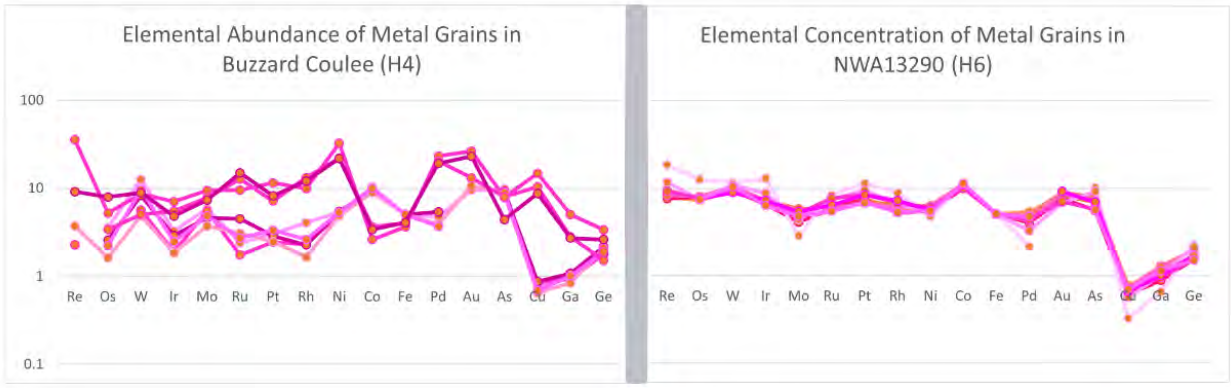

Figure 6. Trace Element Abundance of Metal Grains in H4 and H6 Chondrite. *These are logarithmic plots that record CI normalized abundance of siderophile elements in order of increasing volatility from left to right. The plot to the left represents a type 4 chondrite, and the plot to the right represents a type 6 chondrite.*

Another observation about petrologic type-dependent patterns relates to the presence of Fe-Ni alloys in the metal grains. The metal grains in H chondrites tend to have higher Fe-Ni ratios, meaning they are mostly composed of kamacite. The metal grains in LL chondrites tend to have lower Fe-Ni ratios, so they are mostly composed of taenite. The metal grains found in L and LL chondrites tend to have a mixture of both kamacite and taenite, but there are some H chondrites that can contain both alloys as well, particularly, those of lower petrologic type (Fig. 6).

Fe-Ni Alloys

An unexpected observation made in this study is the significant role of Fe-Ni alloys in the diffusion of siderophile elements. The kamacite member has a high ratio of Fe:Ni (usually under 12 wt. % Ni) while the taenite member has a lower ratio of Fe:Ni (usually over 12 wt. % Ni) (Ramsden et al., 1966). Generally, siderophile elements within each chondrite preferentially diffused into taenite with the exception of Co, As, and W. For ordinary chondrites that contain grains composed of both Fe-Ni alloys, W will preferentially diffuse into either phase depending on the petrologic type of the chondrite (Fig. 7). For example, in an H chondrite that contains both kamacite and taenite, W will preferentially diffuse into the kamacite grains. In an LL chondrite, W will preferentially diffuse into the taenite grains.

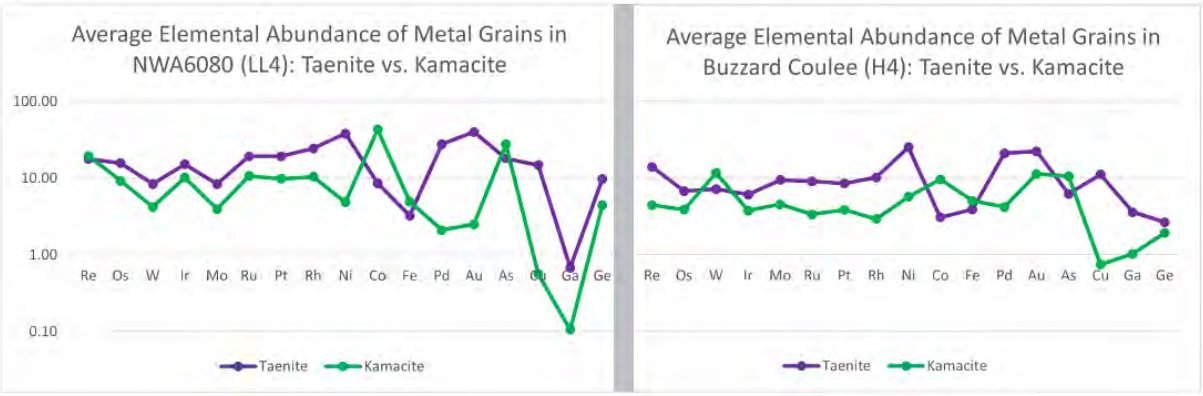

Figure 7. Trace Element Abundance of Metal Grains in LL4 and H4 Chondrite *These are logarithmic plots that record CI normalized abundance of siderophile elements in order of increasing volatility from left to right. The elemental abundance of all the taenite and kamacite grains were averaged in the above plots. Purple = taenite, Green = kamacite*

Grain Size and Distribution

Using size measurements of every metal grain that was analyzed, the trace element abundance data was organized into the size categories defined by Archer et al. (2019); large (>150 microns) and small (<150 microns). At lower metamorphic grades, the small metal grains inherited a higher abundance of siderophile elements than larger metal grains, however, there do seem to be some anomalies in this pattern among Co, As, and W (Fig 8). In chondrites with higher metamorphic grades, siderophile elements are distributed more evenly between small and large metal grains.

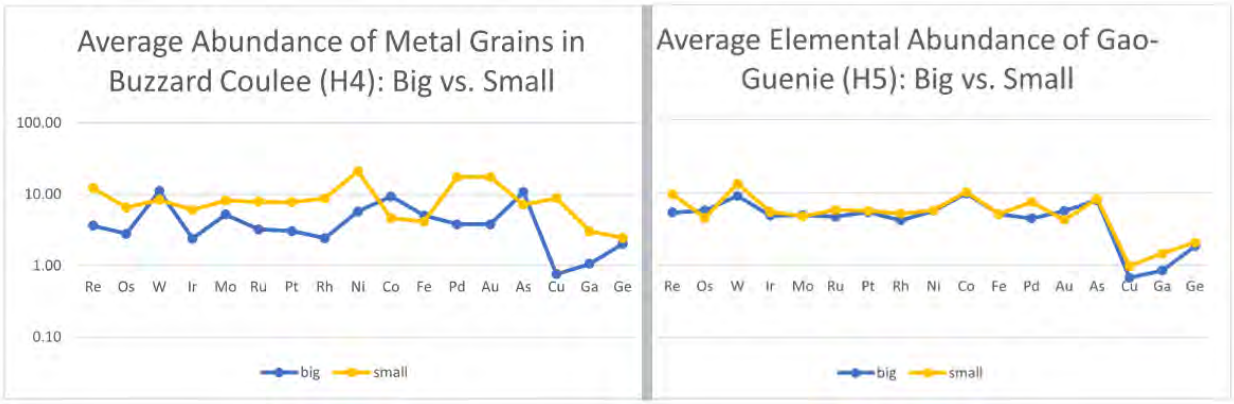

Figure 8. Trace Element Abundance of Metal Grains in H4 and H5 Chondrite *These are logarithmic plots that record CI normalized abundance of siderophile elements in order of increasing volatility from left to right. The elemental abundance of all the large (>150 microns) and small (<150 microns) grains were averaged in the above plots. Blue = big, Yellow = small*

The core and edge of large metal grains was analyzed via laser ablation to learn if there is evidence for zoning, *i.e.*, a tendency for siderophile elements to concentrate in a specific region, or alternatively, if the elemental abundances within grains are homogenized regardless of site location. According to the results, siderophile elements are homogenously distributed in metallic grains, although there does seem to be a slight increase in the abundance of siderophile elements in the edges for some chondrites of low metamorphic grade (Fig. 9).

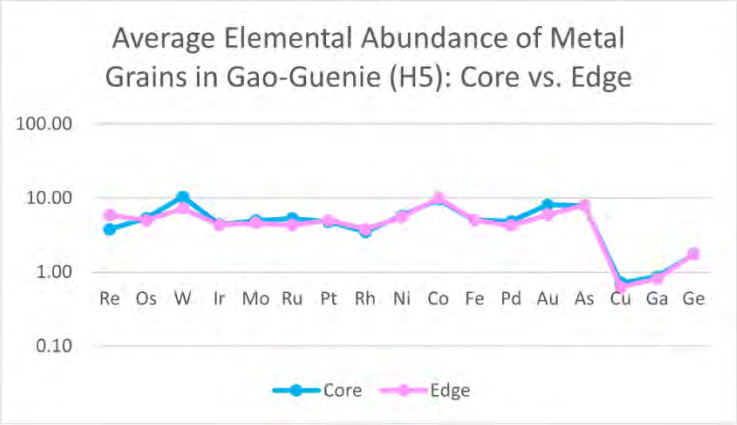

Figure 9. Trace Element Abundance of Metal Grains in H5 Chondrite *This is a logarithmic plot that records CI normalized abundance of siderophile elements in order of increasing volatility from left to right. The elemental abundance of all core and edge analyses were averaged in the above plots. Blue = core, Pink = edge*

Six sites along a transect from edge-to-edge of a large metal grain (2.5mm) within Vinales were analyzed to learn more about the diffusive behavior of siderophile elements inside a single grain (Fig. 10A). The resulting grain profile provides mixed results, as it is inconclusive whether siderophile elements concentrate on the edge, in the core, or anywhere in-between (Fig. 10B). This may be because the composition of very large grains (such as the one used for the grain profile) are a mixture of both kamacite and taenite.

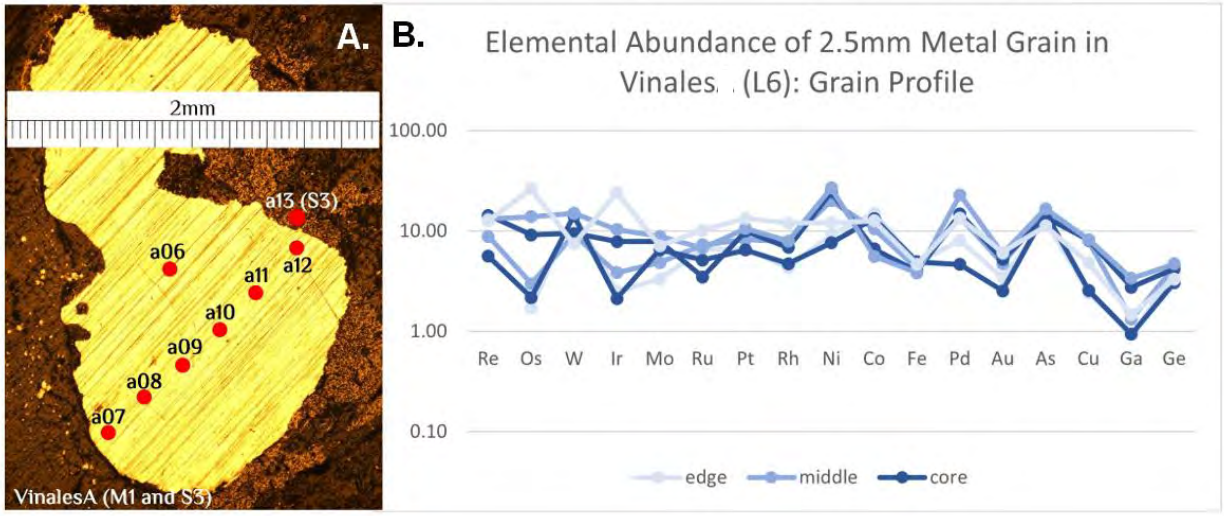

Figure 10. Grain Profile of L6 Chondrite *(B) Logarithmic plot that record CI normalized abundance of siderophile elements in order of increasing volatility from left to right. (A) An annotated image of the analyzed grain and the location of each analysis site.*

Discussion

Reproducibility

In an effort to gauge the reproducibility of our measurements, a Ni/Co ratio graph containing data from the metal grains in H, L and LL chondrites was created (Fig. 11 below). Unfortunately, there are not many resources for in situ research of siderophile elements within the metal grains of ordinary chondrites, however, we were able to find a similar study conducted by Kimura et al. (2008) which used EPMA. When we compare our results to that which was produced by Kimura et al., there are familiar patterns. Both graphs record the Ni/Co ratio of metal grains found in situ within chondritic samples. The Kimura et al. (2008) figure uses L/LL, H/LL, and LL chondrite samples, all of which are type 3 (Fig. 11A). Our figure uses H, L, and LL chondrites that range from type 4 to 6 (Fig. 11B). While the sample ranges differ, the basic concept of comparing the Ni/Co content of metal grains in ordinary chondrites remain the same. The Kimura et al. (2008) data markers display a distinct U-shape with H/LL data in the uppermost left and L/LL data in the uppermost right. Our figure also displays a U-shape pattern with LL4 grains in the uppermost left and LL6 grains in the uppermost right. This is important because finding similarities between our data and that which is found in previous studies gives us confidence in the accuracy and precision of our measurements. This is also an indication that the results found in this investigation can be reproduced.

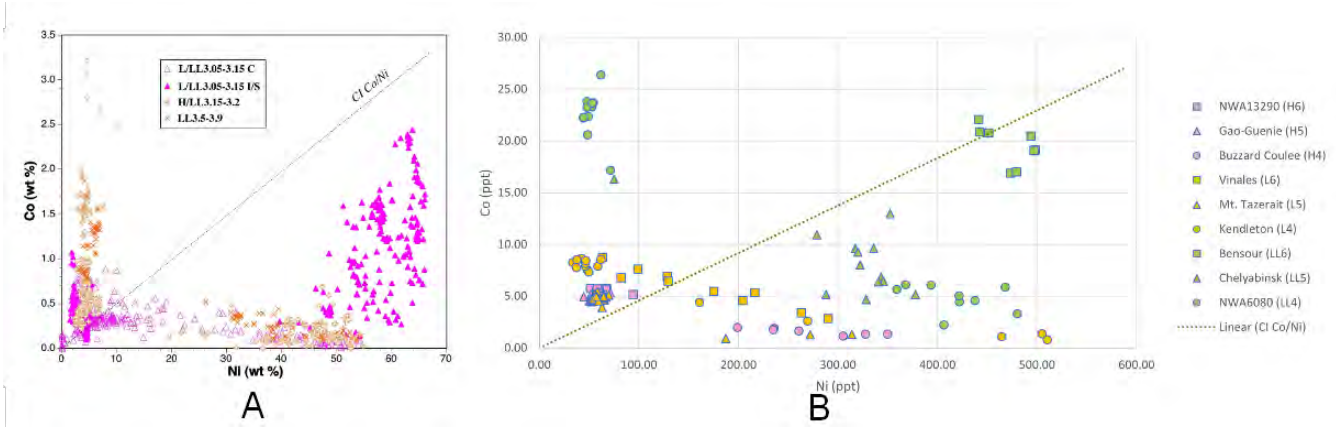

Figure 11. Ni/Co Ratio of Ordinary Chondrites. *(A) figure sourced from Kimura et al. (2008) that plots the Ni:Co ratio of ordinary chondrites by wt. % along with a reference plot of the Ni:Co ratio in CI chondrites. (B) Ni:Co ratio plot created using data from all the metal grains analyzed in this thesis in parts per thousand (ppt) and the ratio of Ni:Co ratio in CI chondrites for reference.*

The Role of Grain Size

According to the results (Fig. 8), grains with a higher surface/volume ratio, which are the smaller grains, tend to contain more siderophile elements than the larger grains. It is also apparent that H chondrites tend to have homogenized grains that "communicate" and operate in a network that evenly distributes material, explaining the uniformity of siderophile abundances between grains (Fig. 5C). Larger grains have the possibility to exhibit zoning, *i.e.*, the concentration of siderophile elements along the edges of the metal grain. However, we found that the difference in abundance between the edges and cores of large metallic grains to be negligible. Therefore, siderophile elements are homogenously distributed within metallic grains, especially those found in high metamorphic type chondrites.

The Role of Fe-Ni Alloys

The abundance graphs that organize grains according to their taenite vs. kamacite compositions suggest that most of the siderophile elements analyzed tend to preferentially diffuse into taenite grains (Fig. 7). There are three elements that do not follow this behavior; Co, As, and W. Cobalt and arsenic preferentially diffuse into kamacite regardless of petrologic type. Tungsten, however, preferentially diffuses into kamacite in reduced (H) chondrites but preferentially diffuses into taenite in oxidized (LL) chondrites. Therefore, tungsten changes its diffusion preferences depending on the oxygen fugacity within the sample. This effect takes priority over the effect of grain size. In Buzzard Coulee (H4), the big metal grains have more tungsten on average than the small metal grains (see Fig. 8). This is because in Buzzard Coulee, the big grains are mostly composed of kamacite, and since this is an H chondrite (most reduced), W preferentially diffuses into kamacite grains. An important detail to note is that while H chondrites tend to contain more kamacite, both alloys can still be present within the sample, and the same goes for LL chondrites.

The Complexity of Siderophile Behavior

While there are some patterns in siderophile behavior, there are also many inconsistencies. For example, H6 chondrites are the most uniform and H chondrites are consistently more uniform than either L or LL chondrites. However, uniformity does not always correlate with metamorphic grade. In H chondrites, uniformity increases with metamorphic grade. In LL chondrites, uniformity seems to decrease as metamorphic grade increases. To be more specific, the most uniform H chondrite analyzed in this study is type 6 but the most uniform LL chondrite analyzed is type 5 (See Fig. 12 below). At this moment, it is hard to tell exactly why the degree of uniformity in the LL chondrites is so inconsistent. However, this is likely due to the particular metamorphic history of each sample. During the interpretation stage, we predicted that perhaps a special heating event occurred during the formation of Chelyabinsk (LL5) that resulted in our sample being more equilibrated than we would expect. Upon further research, we learned that Chelyabinsk experienced high degrees of shock metamorphism and contains silicate melt veins (Grokhovsky et al., 2020). It is possible that the event that caused these characteristics could have also contributed to the equilibration of our sample.

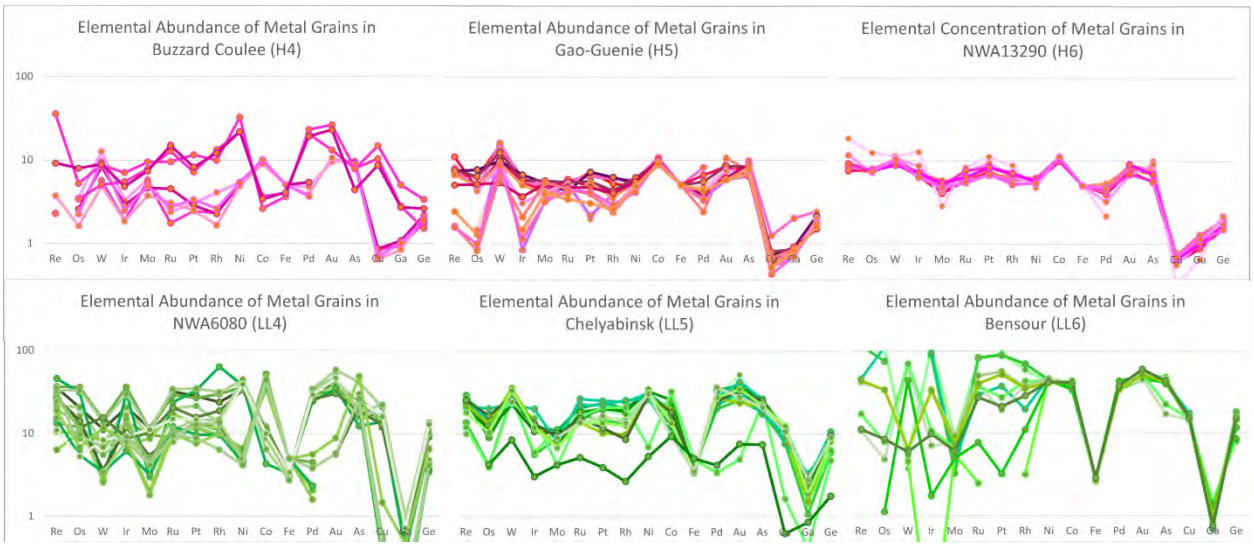

Figure 12. Trace Element Abundance of Metal Grains in H and LL Chondrites. *These are logarithmic plots that record CI normalized abundance of siderophile elements in order of increasing volatility from left to right. Each line characterizes an individual grain. Green = LL, Pink = H. All of the above chondrites range from type 4-6.*

The behavior of siderophile elements is also inconsistent in relation to metamorphic grade. In the H chondrites, all of the siderophile elements become more equilibrated (and uniform) as metamorphic grade increases (Fig. 12, H4-6). In the LL chondrites, however, the volatile elements become more uniform as you increase metamorphic grade, but the refractory elements seem to become less equilibrated (Fig. 12, LL4-6).

Ordinary chondrites have many characteristics that make them unique; no two samples are the same. While siderophile elements have a few consistent patterns of behavior, there are factors that can highlight the individuality of each sample, including but not limited to, the oxidation state of Fe, special events that may have occurred during the sample's thermal metamorphic history, changes in oxygen fugacity, the Fe-Ni alloy within the sample, and the size of the metal grain. Tungsten, in particular, has a complex behavior pattern as it can change what alloy it preferentially diffuses into depending on the oxygen fugacity of the sample (Fig. 7). All things considered, we can see that the behavior of siderophile elements within ordinary chondrites is very complex and dependent upon particular characteristics of each sample.

Conclusion

Our hypotheses proposed that:

I. *Siderophile elements in ordinary chondrites that have experienced a higher degree of thermal metamorphism will be more equilibrated than those that experienced less thermal metamorphism.*
II. *Metal grains that have a higher surface-area/volume ratio, will contain more tungsten than metal grains with a lower ratio*

The results are partially consistent with hypothesis I, as H chondrites become more equilibrated and uniform as the degree of thermal metamorphism increases [type 4 (least equilibrated) < type 5 < type 6 (most equilibrated)]. This is an indication that an increase in thermal metamorphism can drive the diffusion of siderophile elements towards equilibration. However, this pattern of uniformity is not infallibly true for our results for the L or LL chondrites, which have different behavior depending on the volatility of the trace element.

The relationship between grain size and the diffusion of tungsten is consistent with hypothesis II, as the small (<150 micron) metal grains tend to have a higher abundance of siderophile elements than large (>150 micron) metal grains (Fig. 8). Tungsten generally follows this pattern and preferentially diffuses into the small grains, although in Buzzard Coulee (H4), it is more abundant in the big grains (see Fig. 8). However, this is probably because the big grains in this particular sample are mostly composed of kamacite, and since this is an H chondrite (most reduced), tungsten preferentially diffuses into the kamacite.

The results gathered in this study can be applied the findings of the Archer et al. study (2019). They analyzed two H5 chondrites (Forest City and Richardton) that contained small and large metal grains which displayed different Hf-W closure ages. Considering the taenite vs. kamacite results found in this thesis investigation, the varying results found in the Archer et al. study may possibly be due to different Fe-Ni alloys in their samples. This is because tungsten can preferentially diffuse into either alloy depending on the oxygen fugacity within the sample. These changing preferences are likely to alter the measurement of subsequent Hf-W closure ages.

Although the results help us to understand the behavior of W during metamorphism, it is often difficult to distinguish between general principles and behavior in individual samples, as shown by the varying behavior of W in the samples analyzed in the Archer et al. study. This can be remedied by more in situ research of siderophile elements within ordinary chondrites that originate from the same parent body (for example, Chelyabinsk H4-6). If I were to continue this investigation on siderophile behavior in the future, the results can be further constrained by the analysis of more samples from each petrologic type, and an analysis of the H5 chondrites highlighted in the Archer et al. study. Increasing the sample size of ordinary chondrites analyzed would help to distinguish general patterns of siderophile behavior from the individual characteristics of each meteorite.

Bibliography

Archer G., Walker R., Tino J., Blackburn T., Kruijer T., Hellmann J. 2018. Siderophile element constraints on the thermal history of the H chondrite parent body. Geochimica et Cosmochimica Acta 245 pp 556-576

Bouvier, A., Wadhwa, M. 2010. The age of the Solar System redefined by the oldest Pb–Pb age of a meteoritic inclusion. Nature Geoscience 3, pp 637–641

Grokhovsky V., Muftakhetdinova R., Yakovlev G., Brusnitsyna E., Petrova E. 2020. Post-impact metamorphism of the Chelyabinsk meteorite in shock experiment. Science Direct. Planetary and Space Science 192 (20201101)

Grossman J., Brearley A. 2005. The onset of metamorphism in ordinary and carbonaceous chondrites. Meteoritics & Planetary Science 40, Nr 1, pp 87-122

Hellmann J., Kruijer T., Van Orman J., Metzler K., Kleine T. 2019. Hf-W chronology of ordinary chondrites. Science Direct. Geochimica et Cosmochimica Acta pp 258 290-309

Holst J., Olsen M., Paton C., Nagashima K., Schiller M., Wieland D., Larsen K., Connelly J., Jorgensen J., Krot A., Nordlund A., Bizzarro M. 2013. 182Hf-182W age dating of a 26Al-poor inclusion and implications for the origin of short-lived radioisotopes in the early solar system. Proceedings of the National Academy of Sciences of the United States of America v110 n22 (20130528): pp 8819-8823

Horan M., Alexander C., Walker R. 2009. Highly siderophile element evidence for early solar system processes in components from ordinary chondrites. Science Direct. Geochimica et Cosmochimica Acta 73 6984-6997

Huss G., Rubin A., Grossman J. 2006. Thermal metamorphism in chondrites. Meteorites and the Early Solar System II. The University of Arizona Press. pp 576

Kimura, M., Grossman, J. N., Weisberg, M.K. 2008. Fe-Ni metal in primitive chondrites: Indicators of classification and metamorphic conditions for ordinary and CO chondrites. Meteoritics & Planetary Science 43, Nr 7, pp 1161-1177.

Montmerle, T., Augereau, J., Chaussidon, M., Gounelle, M., Marty, B., & Morbidelli, A. 2006. Solar System Formation and Early Evolution: the First 100 Million Years. Earth, Moon, and Planets, 98, pp 39-95.

Ramsden, A. R. 1966. Kamacite and taenite superstructures and a metastable tetragonal phase in iron meteorites. The American Mineralogist. 51: 1–2, 37

Vernazza P., Zanda B., Nakamura T., Scott E., Russell S. 2014. The formation and evolution of ordinary chondrite parent bodies. Asteroids IV. University of Arizona Press. pp 617.

Elemental Abundance of Metal Grains in Buzzard Coulee (H4)

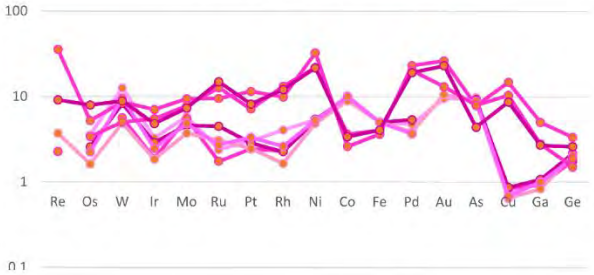

Elemental Abundance of Metal Grains in Gao-Guenie (H5)

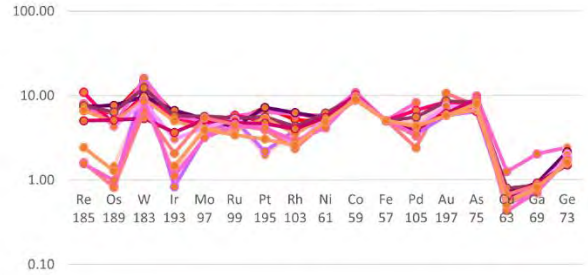

Elemental Concentration of Metal Grains in NWA13290 (H6)

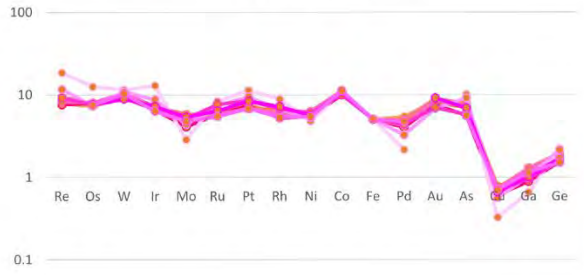

Elemental Abundance of Metal Grains in Kendleton (L4)

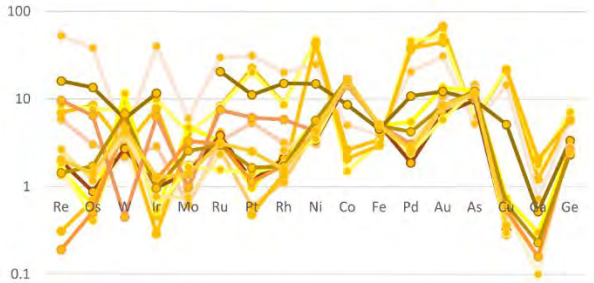

Elemental Abundance of Metal Grains in Mt. Tazerait (L5)

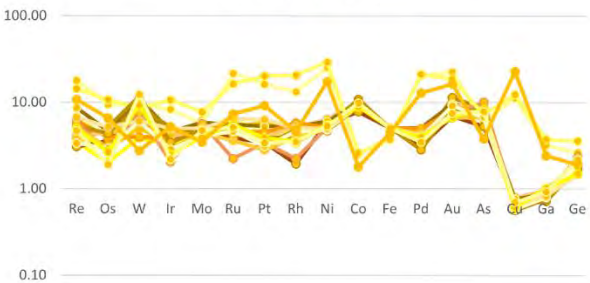

Elemental Abundance of Metal Grains in Vinales (L6)

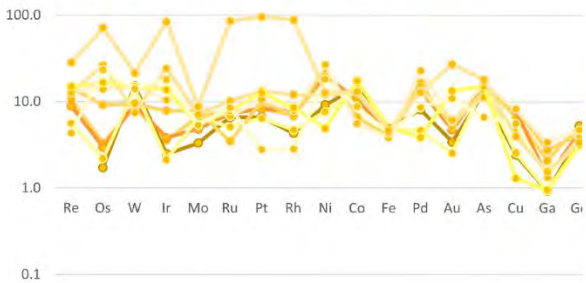

Elemental Abundance of Metal Grains in NWA6080 (LL4)

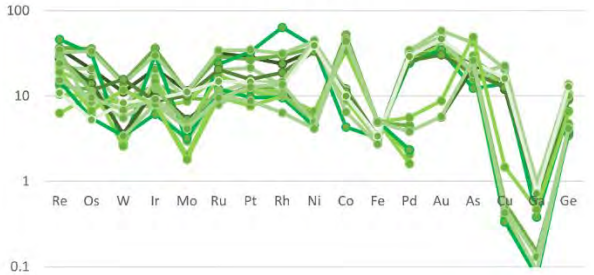

Elemental Abundance of Metal Grains in Chelyabinsk (LL5)

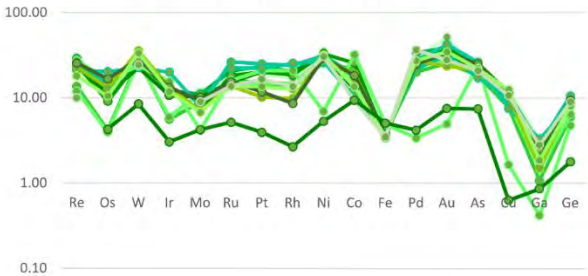

Elemental Abundance of Metal Grains in Bensour (LL6)

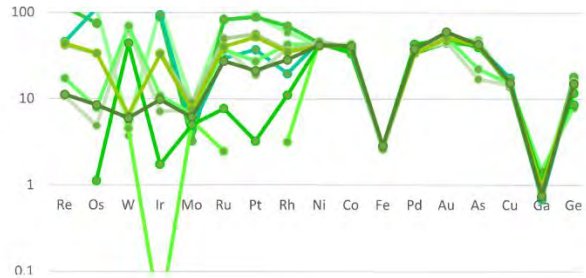

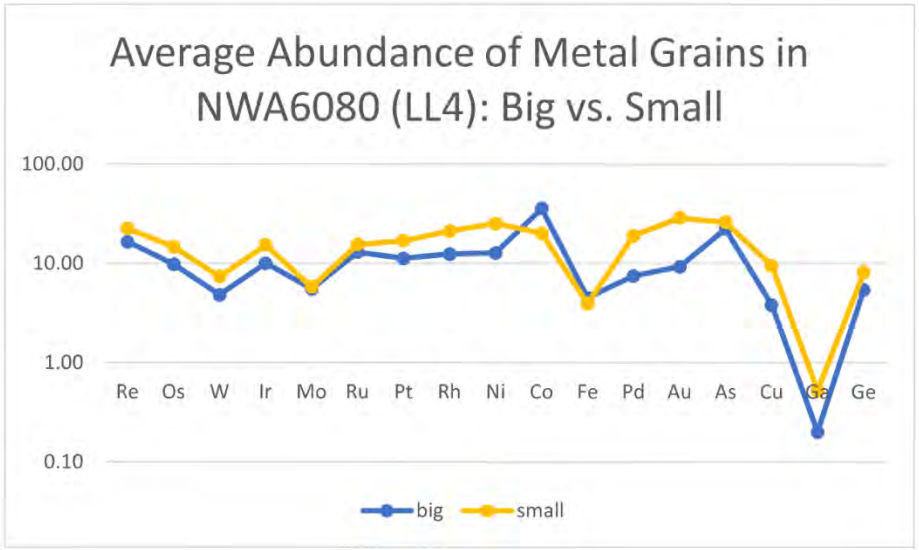
Average Abundance of Metal Grains in NWA6080 (LL4): Big vs. Small
100.00
10.00
1.00
0.10
Re Os W Ir Mo Ru Pt Rh Ni Co Fe Pd Au As Cu Ga Ge
big
small

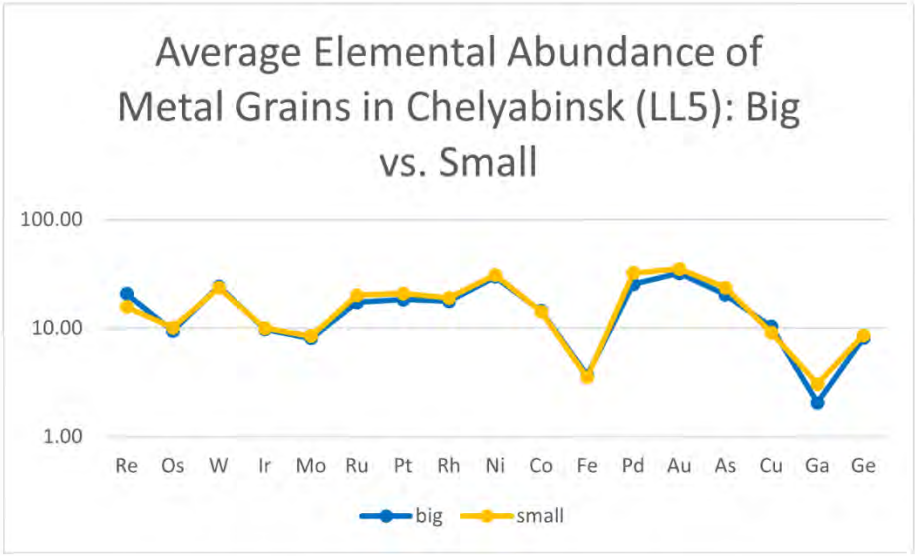
Average Elemental Abundance of Metal Grains in Chelyabinsk (LL5): Big vs. Small
100.00
10.00
1.00
Re Os W Ir Mo Ru Pt Rh Ni Co Fe Pd Au As Cu Ga Ge
big
small

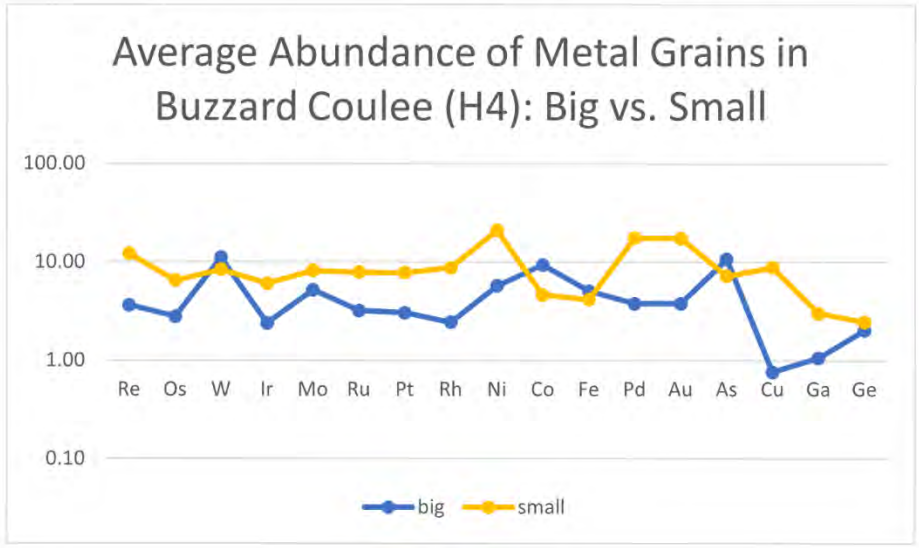
Average Abundance of Metal Grains in Buzzard Coulee (H4): Big vs. Small
100.00
10.00
1.00
0.10
Re Os W Ir Mo Ru Pt Rh Ni Co Fe Pd Au As Cu Ga Ge
big
small

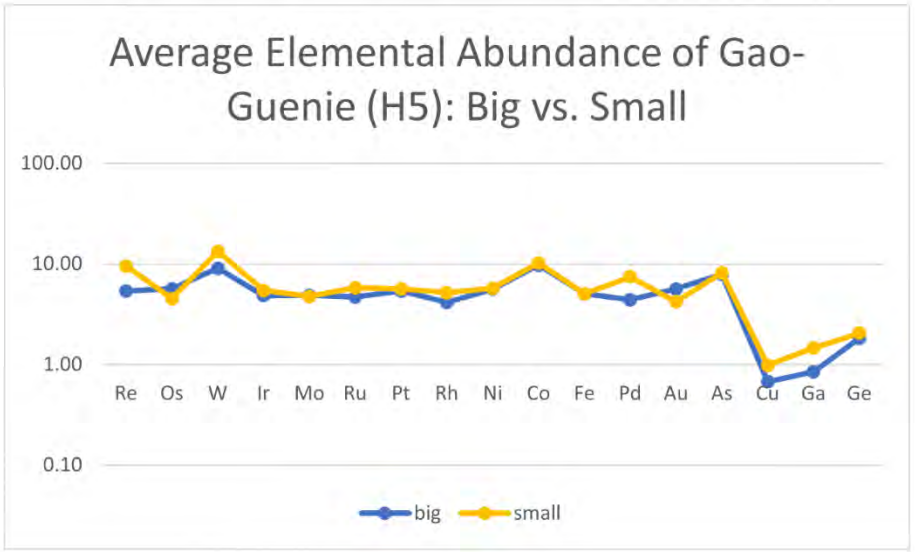
Average Elemental Abundance of Gao-Guenie (H5): Big vs. Small
100.00
10.00
1.00
0.10
Re Os W Ir Mo Ru Pt Rh Ni Co Fe Pd Au As Cu Ga Ge
big
small

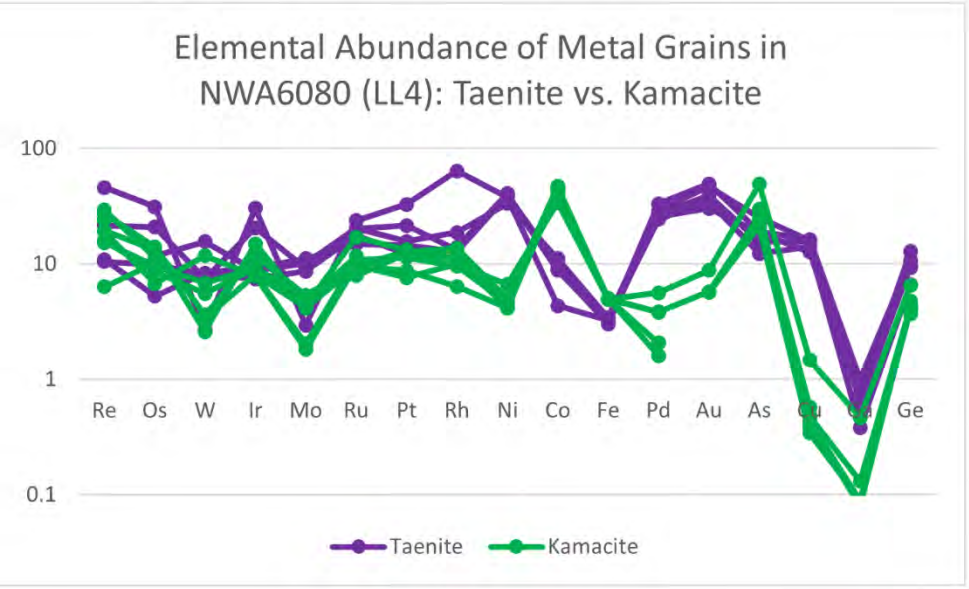
Elemental Abundance of Metal Grains in NWA6080 (LL4): Taenite vs. Kamacite
100
10
1
0.1
Re Os W Ir Mo Ru Pt Rh Ni Co Fe Pd Au As Cu Ga Ge
Taenite
Kamacite

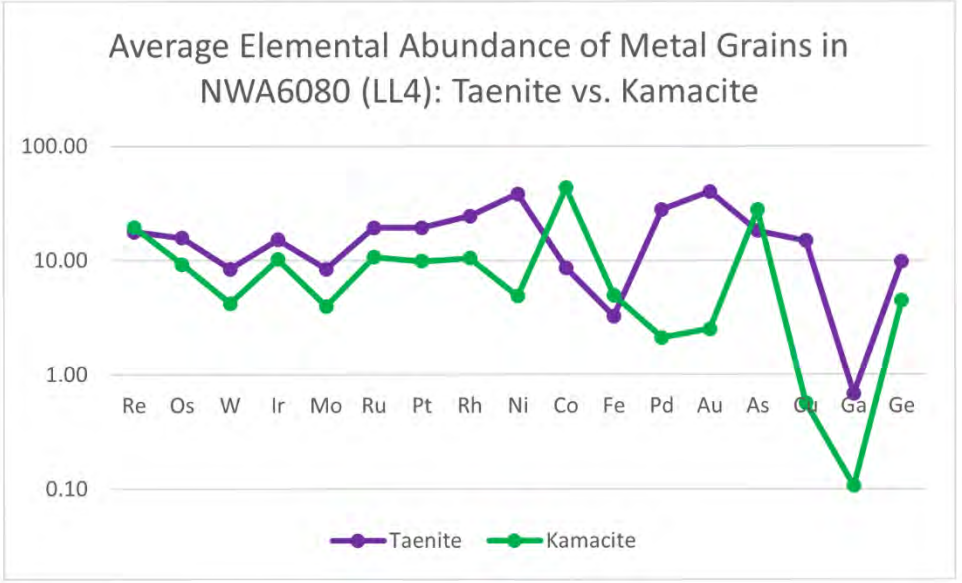
Average Elemental Abundance of Metal Grains in NWA6080 (LL4): Taenite vs. Kamacite
100.00
10.00
1.00
0.10
Re Os W Ir Mo Ru Pt Rh Ni Co Fe Pd Au As Cu Ga Ge
Taenite
Kamacite

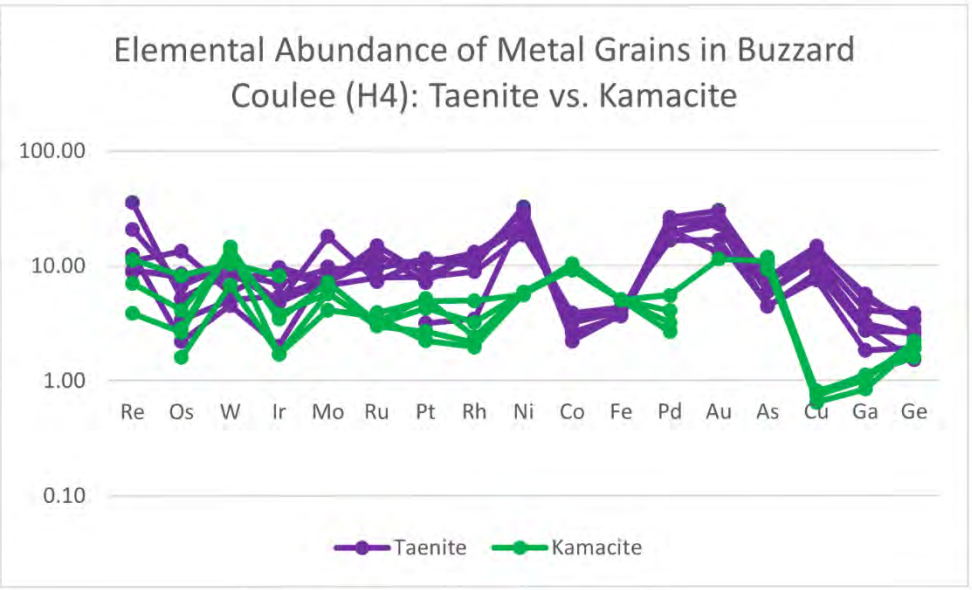
Elemental Abundance of Metal Grains in Buzzard Coulee (H4): Taenite vs. Kamacite
100.00
10.00
1.00
0.10
Re Os W Ir Mo Ru Pt Rh Ni Co Fe Pd Au As Cu Ga Ge
Taenite
Kamacite

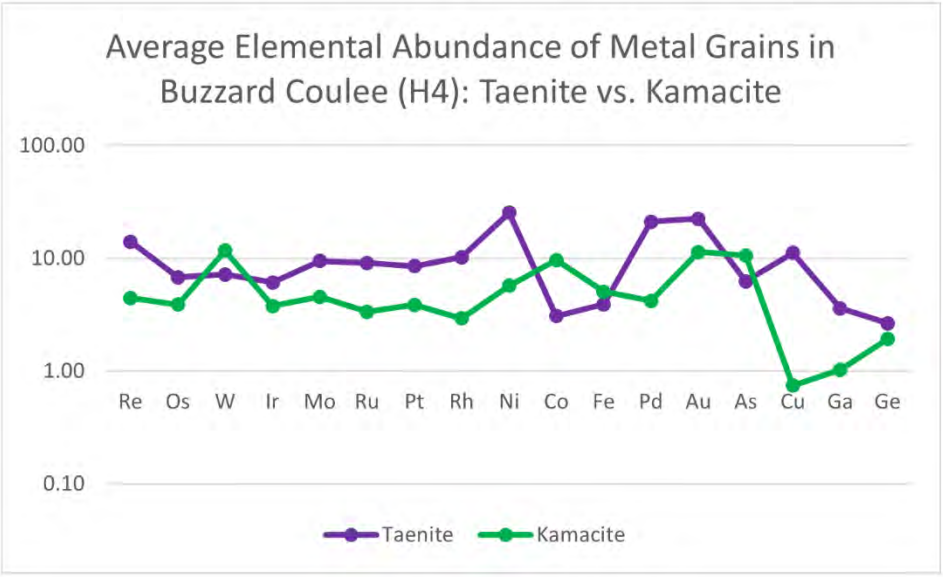
Average Elemental Abundance of Metal Grains in Buzzard Coulee (H4): Taenite vs. Kamacite
100.00
10.00
1.00
0.10
Re Os W Ir Mo Ru Pt Rh Ni Co Fe Pd Au As Cu Ga Ge
Taenite
Kamacite

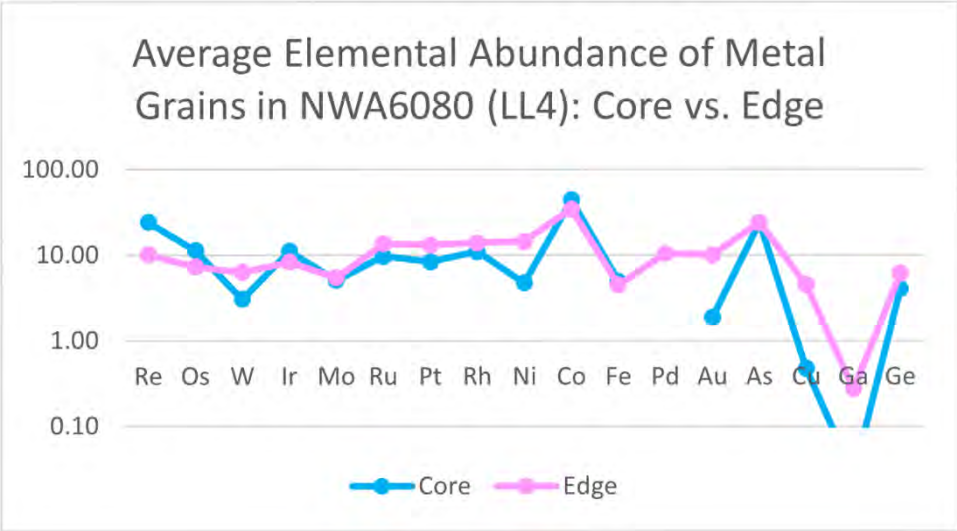
Average Elemental Abundance of Metal Grains in NWA6080 (LL4): Core vs. Edge
100.00
10.00
1.00
0.10
Re Os W Ir Mo Ru Pt Rh Ni Co Fe Pd Au As Cu Ga Ge
Core
Edge

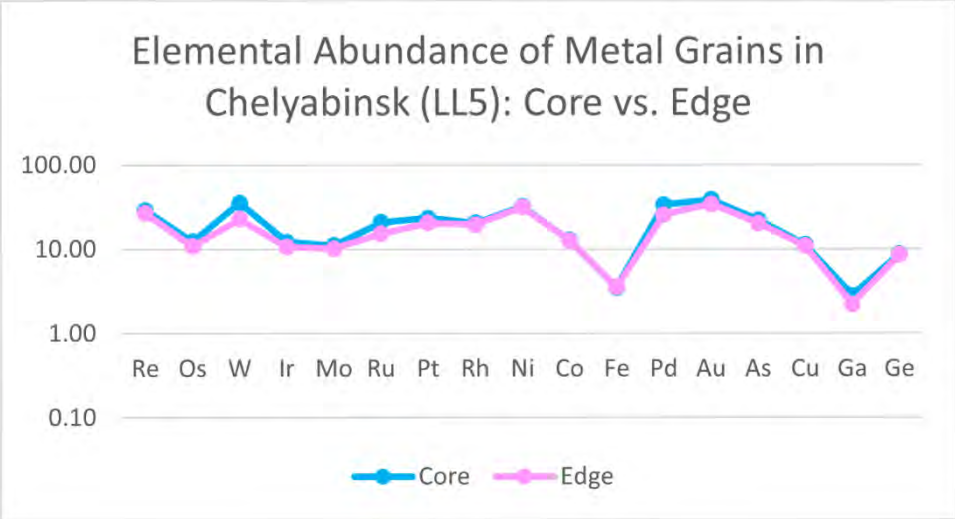
Elemental Abundance of Metal Grains in Chelyabinsk (LL5): Core vs. Edge
100.00
10.00
1.00
0.10
Re Os W Ir Mo Ru Pt Rh Ni Co Fe Pd Au As Cu Ga Ge
Core
Edge

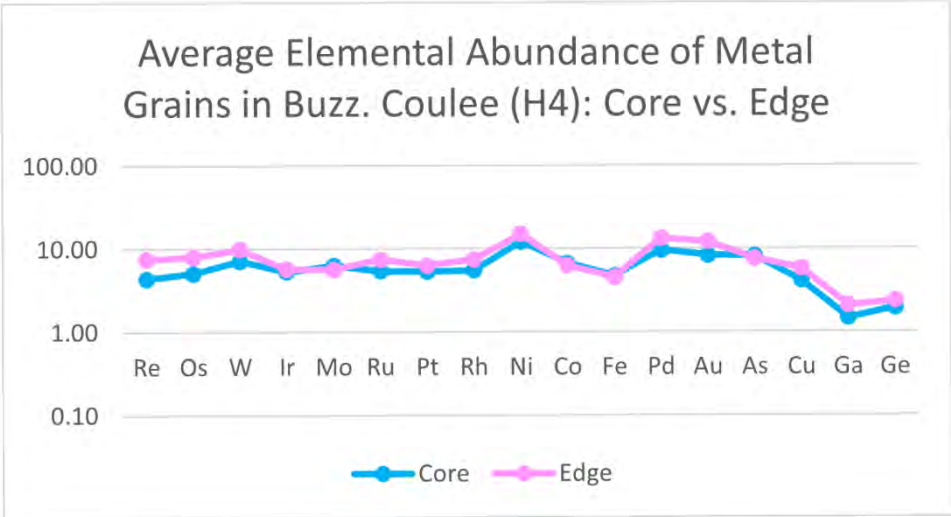
Average Elemental Abundance of Metal Grains in Buzz. Coulee (H4): Core vs. Edge
100.00
10.00
1.00
0.10
Re Os W Ir Mo Ru Pt Rh Ni Co Fe Pd Au As Cu Ga Ge
Core
Edge

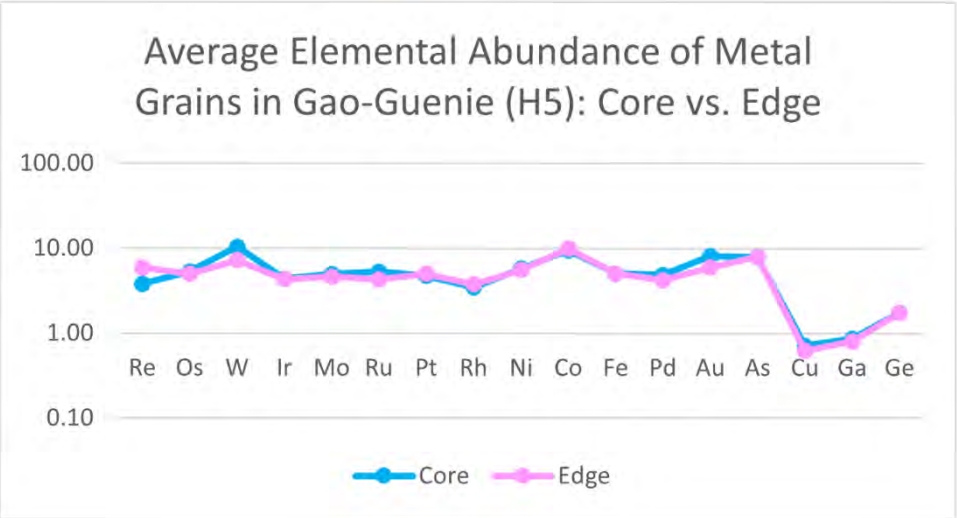
Average Elemental Abundance of Metal Grains in Gao-Guenie (H5): Core vs. Edge
100.00
10.00
1.00
0.10
Re Os W Ir Mo Ru Pt Rh Ni Co Fe Pd Au As Cu Ga Ge
Core
Edge